

# Irisin Attenuates Pathological Neovascularization in Oxygen-Induced Retinopathy Mice

Jieqiong Zhang,<sup>1</sup> Zhifei Liu,<sup>1</sup> Haoqian Wu,<sup>1</sup> Xi Chen,<sup>1</sup> Qiumei Hu,<sup>1</sup> Xue Li,<sup>1</sup> Linlin Luo,<sup>1</sup> Shiyang Ye,<sup>2</sup> and Jian Ye<sup>1</sup>

<sup>1</sup>Department of Ophthalmology, Daping Hospital, Army Medical Center of PLA, Army Medical University, Chongqing, China

<sup>2</sup>State Key Laboratory of Trauma, Burns and Combined Injury, Department of Occupational Disease, Daping Hospital, Army Medical Center of PLA, Army Medical University, Chongqing, China

Correspondence: Shiyang Ye, State Key Laboratory of Trauma, Burns and Combined Injury, Department of Occupational Disease, Daping Hospital, Army Medical Center of PLA, Army Medical University, Chongqing, No. 10, Changjiang Branch, Daping, Yuzhong District, Chongqing 400042, China; [yeshiyang1989@foxmail.com](mailto:yeshiyang1989@foxmail.com).

Jian Ye, Department of Ophthalmology, Daping Hospital, Army Medical Center of PLA, Army Medical University, No. 10, Changjiang Branch, Daping, Yuzhong District, Chongqing 400042, China; [yejian1979@163.com](mailto:yejian1979@163.com).

Received: November 23, 2021

Accepted: June 1, 2022

Published: June 23, 2022

Citation: Zhang J, Liu Z, Wu H, et al. Irisin attenuates pathological neovascularization in oxygen-induced retinopathy mice. *Invest Ophthalmol Vis Sci.* 2022;63(6):21.

<https://doi.org/10.1167/iovs.63.6.21>

**PURPOSE.** Abnormal angiogenesis is a defining feature in a couple of ocular neovascular diseases. The application of anti-VEGFA therapy has achieved certain benefits in the clinic, accompanying side effects and poor responsiveness in many patients. The present study investigated the role of irisin in retinal neovascularization.

**METHODS.** Western blot and quantitative PCR were used to determine irisin expression in the oxygen-induced retinopathy mice model. The pathological angiogenesis and inflammation index were examined after irisin administration. Primary retinal astrocytes were cultured and analyzed for VEGFA expression in vitro. Astrocyte-conditioned medium was collected for transwell assay and tube formation assay in human microvascular endothelial cells-1.

**RESULTS.** Irisin was downregulated in the oxygen-induced retinopathy mice retinae. Additional irisin attenuated pathological angiogenesis, inflammation, and apoptosis in vivo. In vitro, irisin decreased astrocyte VEGFA production, and the conditioned medium suppressed human microvascular endothelial cells-1 migration. Last, irisin inhibited hypoxia-inducible factor-2 $\alpha$ , nuclear factor- $\kappa$ B, and pNF- $\kappa$ B (Phospho-Nuclear Factor- $\kappa$ B) expression.

**CONCLUSIONS.** Irisin mitigates retinal pathological angiogenesis.

Keywords: neovascularization, astrocytes, irisin, OIR

目的:异常的血管生成是新生血管性眼病的显著特征。抗血管内皮生长因子A的治疗在临床上取得了一定的效果,然而同时伴随着不可避免的副作用和不良反应。本研究旨在探讨irisin在视网膜病理性新生血管形成中的作用。

方法:采用免疫印迹和qPCR检测氧诱导视网膜病变小鼠模型中irisin的表达。外源性给予irisin后,检测病理性血管生成和炎症的相关指标。为了研究irisin在体外的作用,我们培养了原代视网膜星形胶质细胞,检测缺氧后VEGFA的表达,并收集星形胶质细胞的条件培养基用于人微血管内皮细胞-1(HMEC-1)的迁移和管腔形成实验。

结果:irisin在氧诱导视网膜病变小鼠视网膜中下调。外源性加入irisin可抑制病理性血管生成、炎症和凋亡。在体外,irisin减少星形胶质细胞中VEGFA的生成,其处理过的星形胶质细胞条件培养基可以抑制人微血管内皮细胞-1的迁移。最后,我们发现irisin可以降低HIF-2 $\alpha$ 、NF- $\kappa$ B和pNF- $\kappa$ B的表达水平。

结论:irisin可减轻视网膜病理性血管生成。

Neovascular eye diseases, including retinopathy of prematurity, diabetic retinopathy (DR), and neovascular AMD, are serious diseases affecting all ages.<sup>1,2</sup> Current studies indicate that their prevalence will continue to increase in the future. Abnormal angiogenesis is a common hallmark and a major cause of visual impairment in these diseases.<sup>1,2</sup> VEGFA plays a master part in the formation of the aberrant vessels and has remained a hotspot since its discovery.<sup>3,4</sup> As a potent angiogenic factor, VEGFA stimulates vascular endothelial cell proliferation and migration.<sup>5</sup> Recent years have witnessed some positive outcomes in anti-VEGFA therapy for neovascular retinal diseases.<sup>6,7</sup> However, the shortcomings, such as poor responsiveness, high cost,

and severe side effects,<sup>7</sup> highlight the need for novel therapies.

Astrocytes, the most abundant cells in the central nervous system and essential components of the neurovascular unit, play critical roles in angiogenesis and neuroinflammation.<sup>8,9</sup> The role of astrocytes in retinal vascularization includes two aspects. One is establishing the physical template for vascular endothelial cell migration, and the other is producing multiple factors that promote and guide angiogenesis.<sup>10,11</sup> A large body of evidence has identified astrocytes as a significant source of VEGFA in both physiological and pathological status.<sup>12,13</sup> During inflammatory responses, astrocytes contribute to the elevated secretion of

proinflammatory factors and sustained microglial activation.<sup>14</sup> Recent research supports that angiogenesis and inflammation are closely coordinated and share multiple signaling mediators in common.<sup>15,16</sup> Promoting inflammation in astrocytes encourages angiogenesis.<sup>17</sup>

Irisin, identified as a myokine in muscle, was initially known for stimulating adipocyte browning and thermogenesis.<sup>18</sup> Current findings implicate that irisin is also secreted in the brain, heart, liver, lung, and other sites.<sup>19,20</sup> Meanwhile, irisin has exhibited various physiological functions, including antiapoptosis, attenuating inflammation, reducing oxidative stress, maintaining the endothelial barrier, and ameliorating mitochondrial dysfunction.<sup>21–23</sup> In the central nervous system, irisin regulates the inflammatory responses by targeting astrocytes.<sup>24–26</sup> Interesting new work in patients with type 2 diabetes mellitus indicates that circulating and vitreous irisin concentrations is correlated with retinopathy development. PDR patients have lower irisin concentrations compared with the controls and patients with type 2 diabetes mellitus without DR.<sup>27–29</sup> These findings raise the possibility that irisin may play a role in retinal angiogenesis.

Our results demonstrate that irisin mitigates pathological neovascularization, suppresses inflammation, and alleviates apoptosis in the OIR mice. In vitro, irisin decreased VEGFA production in cultured astrocytes. Mechanically, irisin reduces the expression levels of hypoxia-inducible factor (HIF)-2 $\alpha$ , nuclear factor (NF)- $\kappa$ B, and pNF- $\kappa$ B (Phospho-Nuclear Factor- $\kappa$ B). Our study suggests that irisin may be a potential therapeutic strategy for neovascular retinal diseases.

## METHODS

### Ethical Approval

Animal welfare was taken into consideration in our experiments. All procedures adhered to the policies and guidelines established by the Military Medical University Animal Care and Use Committee and the ARVO Animal Statement.

### Animals and Experimental Design

C57BL/6J mice were purchased from the animal center of the Daping hospital. All mice were kept in plastic cages with a 12 h light/12 h dark cycle and had free access to food and water. OIR was performed as previously reported.<sup>16</sup> In brief, newborn mice were exposed to 75% oxygen from postnatal day (P) 7 to P12. First, litters were randomly divided into normoxia (mice kept in normal room air) and OIR groups. Mice were sacrificed at P14 and P17 for gene expression studies. Second, littermate OIR mice were randomly divided into OIR + saline and OIR + irisin groups, with normal saline (with 1% dimethylsulfoxide [DMSO]) and irisin (Phoenix Biotechnology, Inc, San Antonio, TX, 42-112) administration. Eyes or retinae were collected for morphological analysis, molecular biology studies, or gene expression studies at P17.

### Irisin Administration

For intravitreal injections, irisin (50 nM, in 1% of DMSO-saline) was given in a final volume of 1  $\mu$ L, systemic treatment with irisin (250  $\mu$ g/kg, intraperitoneal injection) was done twice a day. For cell experiments, irisin was dissolved in PBS (1% of DMSO) and diluted in the medium to a final concentration of 10 nM.

## Whole-Mounted Retinal Immunofluorescence

Mice were perfused with normal saline under anesthetic at P17. The eyes were enucleated and fixated with 4% paraformaldehyde (PFA) for half an hour. After that, intact retinae were dissected and cut into a clover shape under the microscope. The retinae were blocked and permeabilized in normal goat serum containing 3% Triton-X 100 (Sigma-Aldrich, St Louis, MO) overnight at 4°C and incubated with primary antibodies for proliferating cell nuclear antigen (PCNA) (Abcam, Cambridge, UK, ab29), CD31 (Abcam, ab281583), and glial fibrillary acidic protein (GFAP) (CST, #3670) overnight at 4°C. Next, the secondary antibody (Abcam, ab150081) and IB4 (ThermoFisher Scientific, Waltham, MA, 121413) incubation were 24 hours at 4°C. Retinae were washed with normal saline after every step. Finally, retinae were mounted on slides and captured by an Olympus confocal microscopy. Retinal vasculature and astrocyte density were analyzed using AngioTool and Image J software.<sup>16,30,31</sup>

## Immunofluorescence

Eyes were enucleated and fixed overnight in 4% PFA. Next, the eyes were dehydrated in 30% sucrose and embedded in the optimal cutting temperature compound. Then they were fast frozen and cut into 8- $\mu$ m sagittal sections. The sections were permeabilized and blocked with normal goat serum containing 0.5% Triton-X-100 (Sigma-Aldrich) for 1 hour at room temperature. The sections were incubated with primary antibodies irisin (Abcam, ab174833), Tuj 1 (Abcam, ab18207), PCNA (Abcam, ab29), GFAP (Cell Signaling Technology Danvers, MA, #80788), and VEGFA (Proteintech, Rosemont, IL, 66828-1-Ig) overnight at 4°C. After washing in PBS, the sections were incubated with secondary antibodies for 1.5 hours and counterstained with Hoechst (Abcam, ab228551). The sections were observed under an Olympus confocal microscope after being sealed with the fluorescence quenching agent. The colocalization analysis of GFAP with VEGFA was performed employing the colocalization finder plugin of Image J software, as previously described.<sup>32</sup>

## TUNEL Assay

TUNEL staining was performed with a kit (Beyotime, Jiangsu, China, C1089). Retinal sections were fixed in 4% PFA for 30 minutes at room temperature and permeated with cold PBS containing 0.5% Triton X-100 (Sigma-Aldrich) for 5 minutes. After that, the TUNEL reaction agent (Enzyme Solution: Label Solution, 1:9) was added to incubate the sections in a humidified incubator for 1 h at 37°C. Finally, the sections were sealed after Hoechst staining. Fluorescence images were scanned and captured with an Olympus confocal microscope and analyzed with Image J.

## Astrocyte Culture

Astrocytes in the retina were isolated from neonatal pups of C57BL/6J mice following the previous protocol.<sup>33</sup> The astrocyte cultures were seeded in Dulbecco's modified Eagle's medium (DMEM) (Gibco, Waltham, MA) containing 10% fetal bovine serum (Gibco) and maintained in a 95% humidified incubator at 37°C with 5% CO<sub>2</sub>.

## Astrocyte Treatments and Preparation of Astrocyte-Conditioned Medium (ACM)

Astrocytes were incubated with irisin (10 nM) for 24 hours at 80% confluence in the presence or absence of 250  $\mu$ M CoCl<sub>2</sub>

TABLE. Primer Sequences for the Target Genes

Gene	Forward Primer 5'-3'	Reverse Primer 5'-3'
IL-1 $\beta$	GAAATGCCACCTTTTGACAGTG	TGGATGCTCTCATCAGGACAG
MCP-1	ACTGAAGCCAGCTCTCTTCCTC	TTCTTCTTGGGGTCCAGCACAGAC
TNF- $\alpha$	TGCCTATGTCTCAGCCTCTTC	GGTCTGGGCCATAGAACTGA
$\beta$ -Actin	TGTGACGTTGACATCCGTAAA	GTACTIONTGGCTCAGGAGGAG
irisin	GGACTCTTGAAAACACCACTG	TCCACACAGA TGA TCTCACCAC
VEGFA	ATGCGGATCAAACCTCACAAA	TTCTGGCTTTGTCTGTCTTTCTTT

MCP-1, monocyte chemoattractant protein-1.

(Sigma-Aldrich, in DMEM). The naïve control (NC) received the same volume of PBS (1% DMSO). For integrin inhibitor treatment, cells were treated with 100 ng/mL RGD peptide (MCE, HY-P1740, in DMEM) in the presence or absence of irisin (10 nM) upon exposure to 250  $\mu$ M CoCl<sub>2</sub>. After the treatments, the conditioned medium was collected for the following ELISA test and HMECs-1 incubation. Cold PBS was added to the astrocytes. RLS or radioimmunoprecipitation assay buffer for lysis were added after PBS aspiration for quantitative PCR (qPCR) and Western blot analysis. The astrocytes conditioned medium was 1:1 mixed with fresh medium for the transwell migration assay and tube formation assay in HMECs-1.

### ELISA

Free VEGFA in astrocyte conditioned medium was measured by a VEGFA ELISA Kit (Cloud-Clone Corp, Houston, TX, SEA143Mu) according to the manufacturers' instructions. All samples were collected on ice and centrifuged at 1000g for 5 minutes at 4°C to remove the cell debris. The optical density value was measured at 450 nm wavelength.

### Transwell Migration Assay

HMECs-1 (American Type Culture Collection, Manassas, VA; CRL-3243) were seeded in DMEM supplemented with 5% fetal bovine serum in the upper chamber of transwell insets (Corning, Corning, New York) (8- $\mu$ m pore) in 24 plates. ACM or fresh medium was placed in the bottom chamber. After 24 hours in culture, the membranes were washed with PBS and fixed with 4% PFA. After wiping cells off the upper side of the membrane with a cotton swab, the membranes were detached, stained with violet crystalline, and mounted on slides. Randomly selected fields were captured by an optical microscope and analyzed with Image J software.

### Tube Formation Assay

Matrigel (BD Biosciences, Franklin Lakes, NJ) was coated on 24-well culture plates and polymerized for 30 minutes at 37°C. HMECs-1 ( $2 \times 10^4$  cells) were seeded on the surface of the Matrigel and treated with ACM or fresh medium for 6 hours. For VEGFA supplementation, approximately 140 pg/mL VEGFA (Abcam, ab185265) was added in the ACM. The formed tubes were observed and photographed. Tube formation was quantified in randomly selected fields with angiogenesis analyze plugin of Image J software.

### Protein Extraction and Western Blot Analysis

Retinae and astrocytes from different groups were harvested at other times accordingly. Protein was extracted by radioimmunoprecipitation assay containing protease inhibitors. After centrifuging at 10,000g for 15 minutes at 4°C, the supernatants were collected. A BCA kit (Beyotime, P0010) was used to measure the concentrations. The proteins with

loading buffer were heated to 100°C for 10 minutes. Equal amounts of protein were resolved on SDS-PAGE Gel under 120 V and transferred to polyvinylidene difluoride filter membrane (Millipore, Bedford, MA). Blocked with 5% BSA in TBS-Tween 20 for 1 h at room temperature, the polyvinylidene difluoride filter membranes were incubated with irisin (Abcam, ab174833), PCNA (Abcam, ab29), VEGFA (Abcam, ab46154), caspase 3 (Bioss, Woburn, MA, bsm-33284M), HIF-2 $\alpha$  (CST, #57921), NF- $\kappa$ B (CST, #8242), p-NF $\kappa$ B (CST, #3033),  $\beta$ -actin (CST, #3700), and glyceraldehyde-3-phosphate dehydrogenase (CST, #5174) antibodies in antibody dilution solution overnight at 4°C. On the following day, after washing three times, the polyvinylidene difluoride filter membranes were incubated with the secondary antibody (CST, 7076/7) for 1.5 hours and visualized by an enhanced chemiluminescence system (Millipore).

### qPCR

RNA was extracted using the universal RNA extraction kit (Accurate Biology, AG21022, Hunan, China) and converted to cDNA by using Evo M-MLVRT Premix for qPCR (Accurate Biology, AG11701). qPCR was conducted according to the manufacturer's protocol, using the SYBR Green RT-PCR Master mix.  $\beta$ -Actin was used as an internal control to normalize the target gene expressions. The  $2^{-\Delta\Delta CT}$  method was used to calculate the gene expression. The PCR primers are listed in Table. The condition for the reaction was 95°C for 45 seconds, 60°C for 30 seconds to denaturation, and 72°C for 45 seconds for 40 cycles to extension. All experiments were performed in triplicate.

### Statistical Analysis

All data were expressed as mean  $\pm$  standard error of the mean. A *P* value of less than 0.05 was considered statistically significant. The Student *t* test was used when two groups were compared. One-way ANOVA followed by Tukey multiple comparisons was used when three or more groups were compared. Statistical analyses were performed with GraphPad Prism (GraphPad Software Inc, San Diego, CA).

## RESULTS

### Irisin Is Downregulated in the Oxygen-induced Retinopathy (OIR) Mice Model

OIR is a popular model for studying pathological angiogenesis in the retina, because it can mimic the cardinal features of retinopathy of prematurity and proliferative DR.<sup>34</sup> The establishment of the OIR model was illustrated in Figure 1A. To investigate the potential role of irisin in retinal neovascularization, we measured the levels of irisin in the OIR mice at first. qPCR revealed that the OIR retinae had a decrease in the irisin mRNA expression at P14 and P17, and the

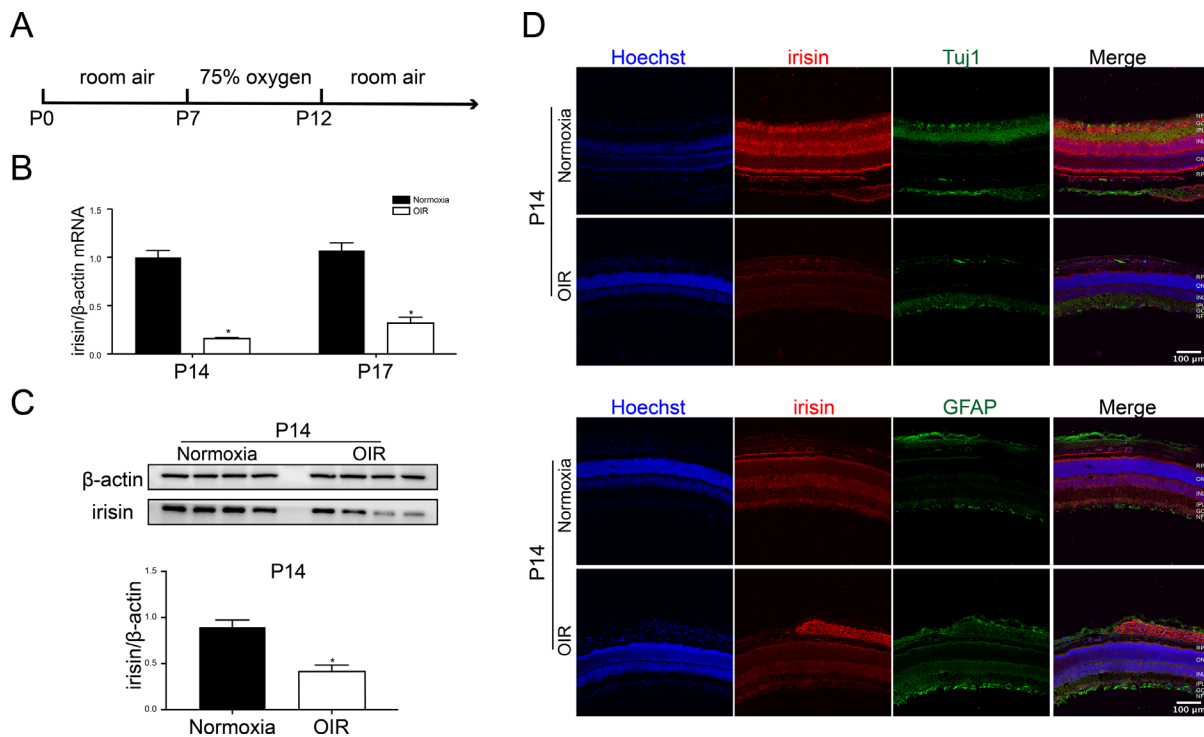


**FIGURE 1.** Irisin is decreased in the retinae of the OIR mice. **(A)** Diagrammatic illustration of the OIR mice model. **(B)** A qPCR analysis of irisin mRNA expression in normoxic and OIR retinae at P14 and P17. Data were normalized to gene expression of the normoxia group, and  $\beta$ -actin was used as an internal control ( $n = 3-4$ ). **(C)** Western blot analysis and quantification of irisin in normoxic and OIR retinae at P14 ( $n = 4$ ). **(D)** Representative immunofluorescence images of irisin (red) and GFAP (green) in P14 normoxic and OIR mice retina cryosections. Scale bar, 100  $\mu\text{m}$ . \* $P < 0.05$ . GCL, ganglion cell layer; INL, inner nuclear layer; IPL, inner plexiform layer; NFL, nerve fiber layer; ONL, outer nuclear layer.

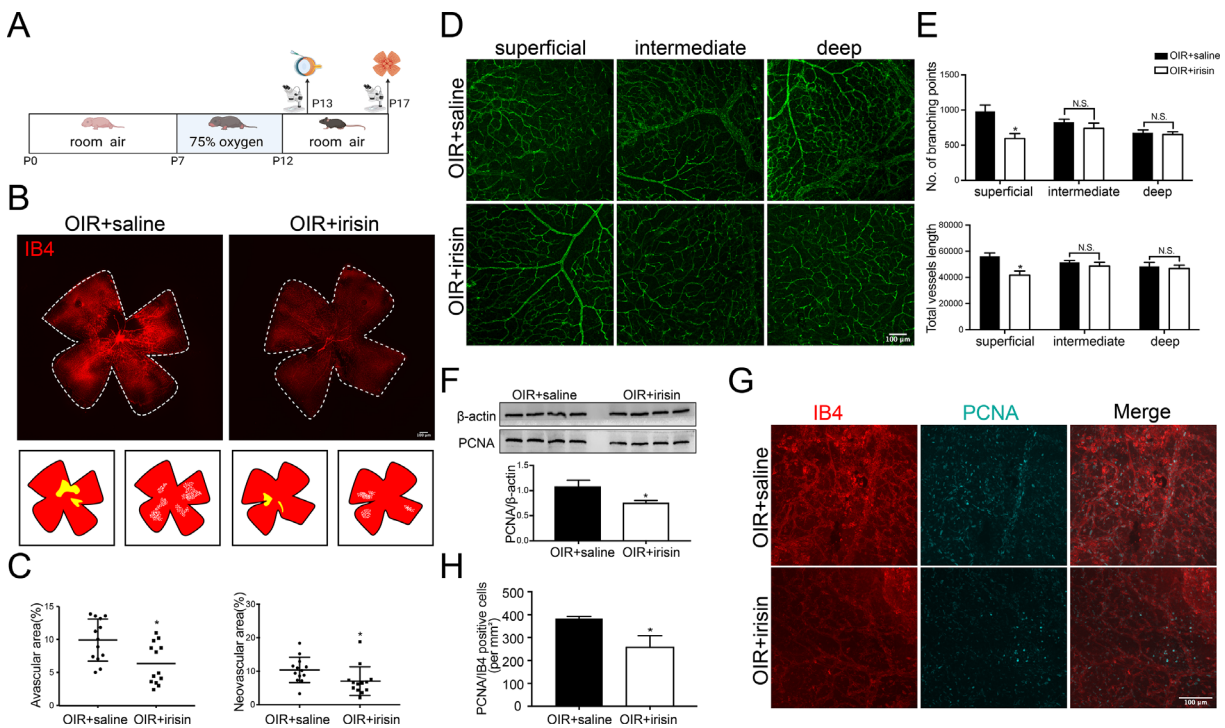


**FIGURE 2.** Supplementation of irisin alleviates aberrant angiogenesis in OIR mice. **(A)** Irisin or saline was administered to the OIR mice via vitreous injection at P13, and retinae were analyzed at P17. **(B)** IB4 staining of whole-mount retinae from OIR + saline and OIR + irisin mice at P17. The yellow area indicates the avascular area in the insets, and the white area indicates the neovascular area. **(C)** Quantification of the avascular area and neovascular area at P17 in OIR + saline and OIR + irisin mice retinae, related to **(B)**. **(D and E)** Representative images of CD31 (green) in superficial, intermittent, and deep retinal layers in OIR + saline and OIR + irisin mice retinae at P17, with quantification of the vessel length and branching points of superficial, intermediate, and deep vascular network ( $n = 7-8$ ). **(F)** Western blot analysis and quantification of PCNA protein in the retinae of OIR + saline and OIR + irisin mice. **(G and H)** Representative images and the corresponding quantification of PCNA<sup>+</sup>/IB4<sup>+</sup> cells in OIR + saline and OIR + irisin mice ( $n = 3-4$ ). \* $P < 0.05$ .

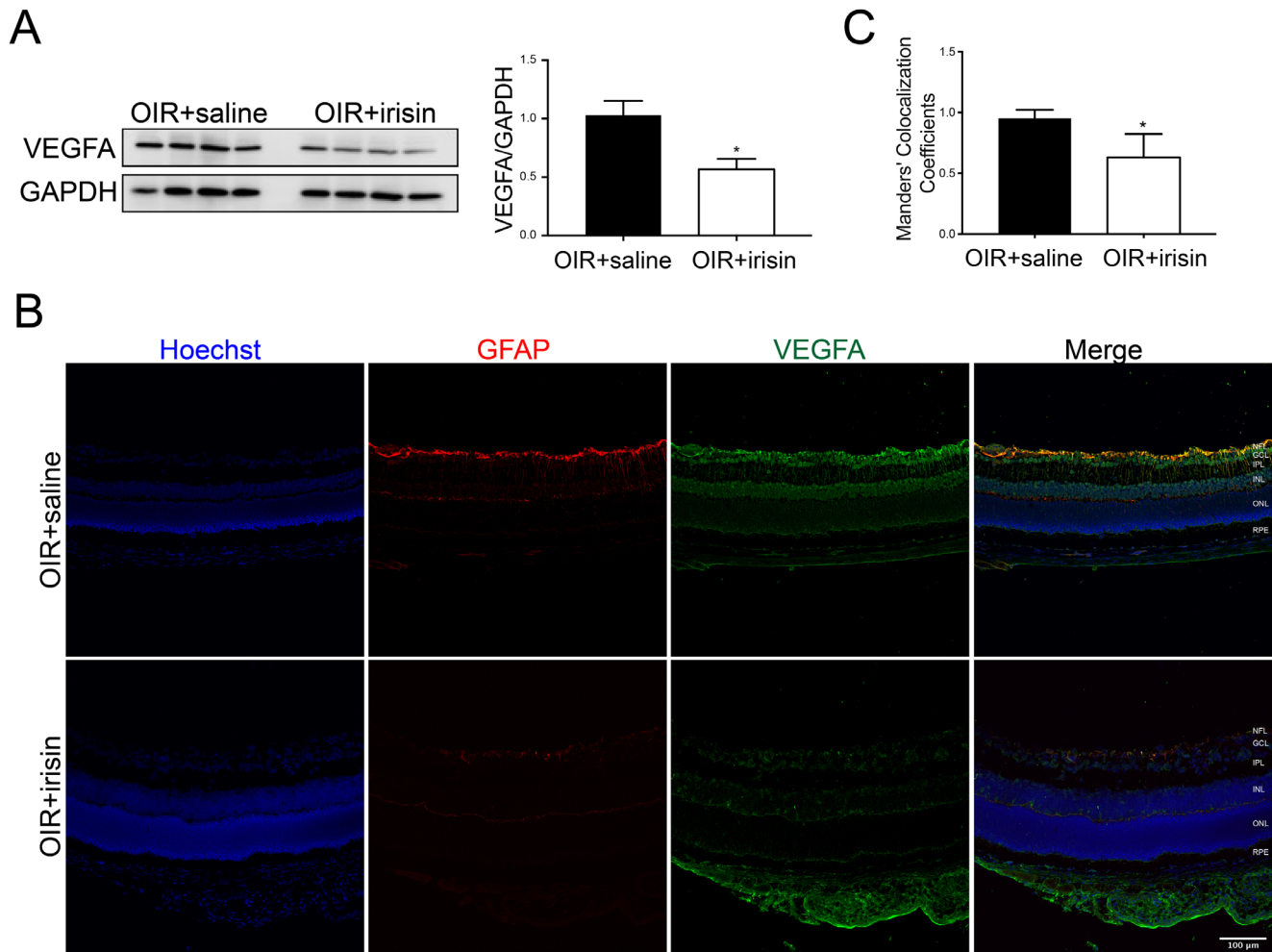


**FIGURE 3.** VEGFA is downregulated by irisin administration in OIR mice. **(A)** Western blot analysis and quantification of VEGFA in OIR + saline and OIR + irisin retinæ at P17 ( $n = 7$ ). **(B)** Representative images of retinal cryosection staining with VEGFA (green) and GFAP (red) in OIR + saline and OIR + irisin mice at P17. **(C)** Fluorescence signal intensities of VEGFA and GFAP containing quantified from OIR + saline and OIR + irisin group, related to **(B)** ( $n = 4-5$ ). GCL, ganglion cell layer; INL, inner nuclear layer; IPL, inner plexiform layer; NFL, nerve fiber layer; ONL, outer nuclear layer.

decrease was more evident at P14 (Fig. 1B). Hence, we examined the protein expression of irisin at P14, and the results confirmed that irisin was significantly decreased in the OIR group (Fig. 1C). Immunofluorescence further ascertained the existence of irisin, mainly in the nerve fiber layer, inner plexiform layer, and RPE layer (Fig. 1D). Because there was a negative relationship between irisin and VEGFA in clinical patients with DR,<sup>35</sup> we also examined the expression of VEGFA at P14. Western blot indicated that VEGFA was increased in the OIR group (Supplementary Fig. S1). These results offer a rationale for further exploring the function of irisin in retinal neovascularization.

### Irisin Mitigates Pathological Neovascularization in OIR Mice

To explore the effects of irisin in pathological angiogenesis, we administered it to the OIR mice via either intravitreal (Fig. 2A) or intraperitoneal injection (Supplementary Fig. S2). Wholemount immunostaining with IB4 showed that both neovascular area (OIR + saline group,  $10.4 \pm 1.05\%$ ; OIR + irisin group,  $7.03 \pm 1.19\%$ ; a 32.4% decrease)

and avascular area (OIR + saline group,  $9.89 \pm 0.88\%$ ; OIR + irisin group,  $6.3 \pm 0.86\%$ ; a 36.2% decrease) were significantly decreased after irisin administration (Figs. 2B, 2C). Also, the vessel lengths and the number of branching points in each layer were measured. Results showed that irisin slightly decreased the vessel lengths and the number of branching points in the superficial plexus compared with the OIR + saline group (Figs. 2D, 2E). To confirm these results, we performed a Western blot analysis and wholemount staining to detect the expression of PCNA, a vascular endothelial cell proliferative marker.<sup>16</sup> The results displayed that irisin decreased the expression of PCNA protein (Fig. 2F). Meanwhile, PCNA/IB4 positive cells in the neovascular area decreased by 33% in the OIR + irisin group compared with the OIR + saline group (Figs. 2G, 2H).

### Irisin Reduces VEGFA Expression in the OIR Mice Model

Owing to the pivotal role of VEGFA in angiogenesis and the inverse correlation between irisin and VEGFA, we further analyzed the expression of VEGFA in the retinæ after

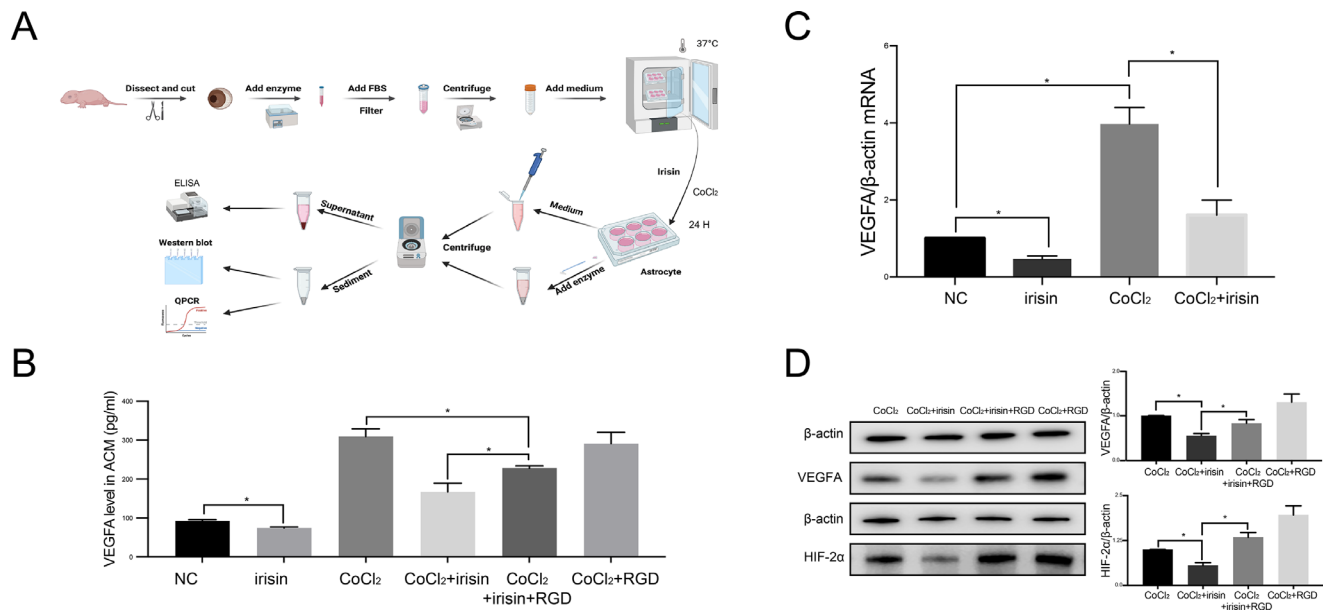


**FIGURE 4.** Irisin impairs hypoxia induced VEGFA production in astrocytes in vitro. **(A)** Schematic illustration of astrocytic preparations for ELISA, Western blot, and qPCR. Astrocytes were exposed to 250  $\mu$ M CoCl<sub>2</sub> in the absence or presence of irisin (10 nM) and/or RGD peptide (100 ng/mL) for 24 hours. The NC group was treated with the same volume of the solvent PBS (1% DMSO). **(B)** Free VEGFA concentrations in conditioned media from primary astrocytes were determined by ELISA. **(C)** A qPCR analysis of VEGFA mRNA expression in astrocytes from NC, irisin, CoCl<sub>2</sub> and CoCl<sub>2</sub> + irisin groups. **(D)** Western blot analysis and quantification of VEGFA and HIF-2 $\alpha$  protein level in astrocytes from CoCl<sub>2</sub>, CoCl<sub>2</sub> + irisin, CoCl<sub>2</sub> + irisin + RGD, and CoCl<sub>2</sub> + RGD groups ( $n = 4$ ). \* $P < 0.05$ .

intravitreal injection of irisin. Western blot showed that VEGFA expression was reduced nearly by one-half in the OIR + irisin group (Fig. 3A). However, VEGFA significantly increased in the OIR mice compared with those kept in room air simultaneously (Supplementary Fig. S3). Because astrocytes have been proved to be a major source of VEGFA during hypoxia, we conducted double immunofluorescent staining of GFAP and VEGFA. Colocalization analysis revealed that the intensity of GFAP and VEGFA costaining was mitigated by irisin in OIR mice (Figs. 3B, 3C). These results further suggest that irisin may exert its antiangiogenic effect by targeting astrocytes.

### Irisin Inhibits VEGFA Production in Cultured Astrocytes upon Hypoxia Stimulus

Later, we carried out in vitro experiments to exclusively observe the effect of irisin on astrocytes. Primarily cultured astrocytes were treated with CoCl<sub>2</sub> (a chemical hypoxic agent) to simulate hypoxia insult.<sup>36</sup> ELISA, qPCR, and Western blot analyses were conducted to detect VEGFA secretion and expression in the astrocytes (Fig. 4A). ELISA results revealed that the concentration of VEGFA in the medium was higher in the CoCl<sub>2</sub> group than in the NC group. Irisin decreased the VEGFA concentration in astrocytes with or without CoCl<sub>2</sub> (Fig. 4B). Likewise, the mRNA levels of VEGFA were decreased by irisin in the presence or absence of CoCl<sub>2</sub> (Fig. 4C). RGD peptide, an integrin receptor inhibitor,<sup>37</sup> inhibits the effect of irisin on astrocyte VEGFA secretion and expression in CoCl<sub>2</sub> treated astrocytes. We also detected the protein expression of HIF-2 $\alpha$ , an important regulator of VEGFA. Results indicated that HIF-2 $\alpha$  was downregulated by irisin, whereas RGD cotreatment reversed this inhibitory effect (Fig. 4D).

### Conditioned Medium From Irisin-pretreated Astrocytes Suppresses HMECs-1 Migration

To further clarify the linkage between irisin and astrocyte in retinal angiogenesis, we collected ACM from the NC, irisin, CoCl<sub>2</sub>, and CoCl<sub>2</sub> + irisin groups in Figure 4 to incubate HMECs-1. Fresh media corresponding with these four groups were set up to exclude the direct effect of irisin on HMECs-1 (Fig. 5A). When HMECs-1 were cultured in fresh medium, we found no significant difference in the number of migrated cells between the NC and the irisin groups. However, the number of migrated HMECs-1 in the irisin ACM group ( $90.00 \pm 5.80$ ) was significantly decreased compared with the NC ACM group ( $120.00 \pm 1.29$ ) (Figs. 5B, 5C). Similarly, there was no significant difference in tube formation between the CoCl<sub>2</sub> and the CoCl<sub>2</sub> + irisin groups when HMECs-1 were cultured in fresh medium. However, the vessel length per field in the CoCl<sub>2</sub> + irisin ACM group is 70% of the CoCl<sub>2</sub> ACM group. In addition, VEGFA supplementation (the difference between CoCl<sub>2</sub> and CoCl<sub>2</sub> + irisin ACM) to the CoCl<sub>2</sub> + irisin ACM partly restored irisin's inhibitory effect on HMECs-1 tube formation (Figs. 5D, 5E).

### Irisin Decreases HIF-2 $\alpha$ Expression in the Retinae of OIR Mice

Western blot analysis indicated that HIF-2 $\alpha$  was decreased by irisin administration in OIR mice (Fig. 6A). Except for VEGFA secretion, another critical role for astrocytes is establishing the physical scaffold for vessel migration. The deletion of astrocytes results in aberrant angiogenesis, and the density of astrocytes has been observed to decrease in OIR and DM mice retinae.<sup>38-40</sup> Here, we showed that the astrocyte density was increased in the OIR + irisin group

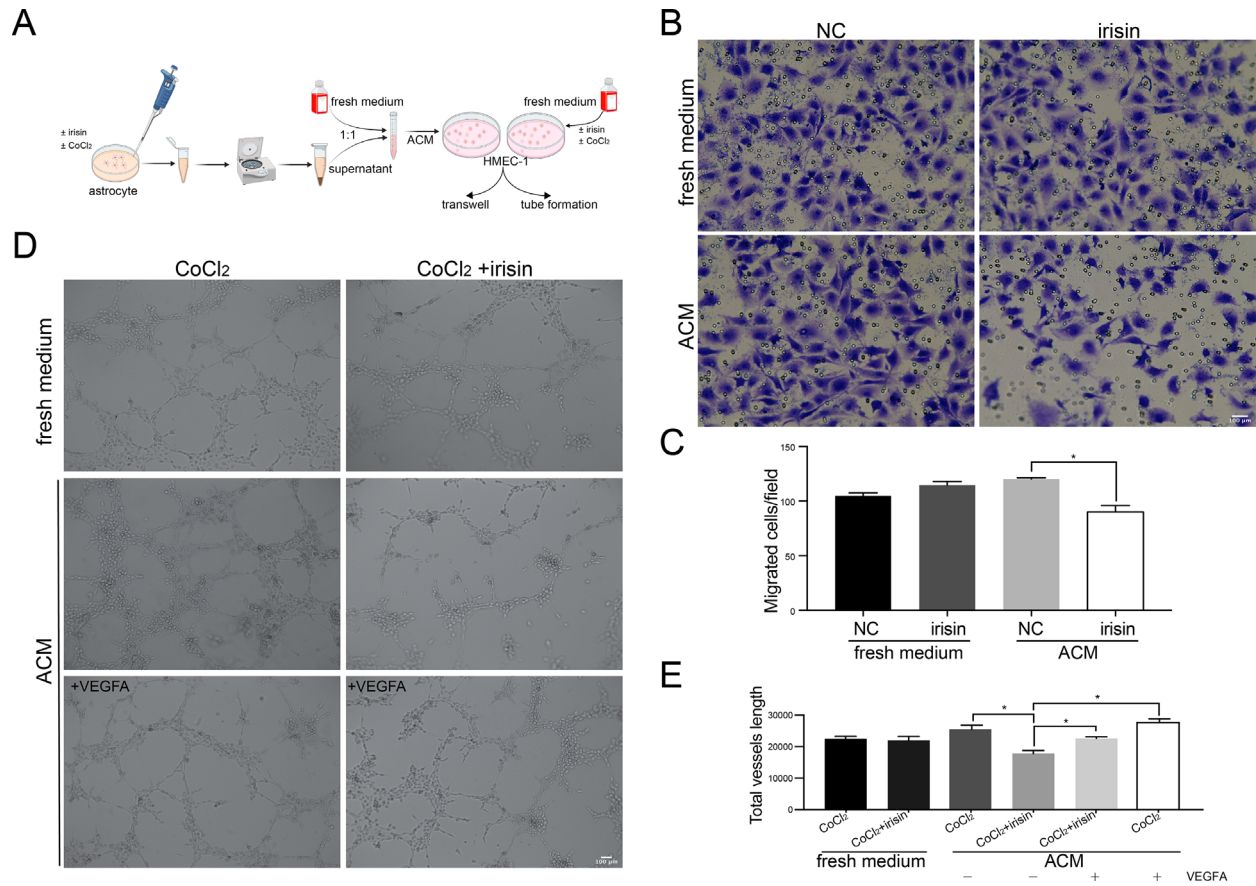


**FIGURE 5.** Effects of ACM from different groups on HMECs-1 migration and tube formation. **(A)** Schematic illustration of cell experiments. **(B)** Representative images of HMECs-1 transwell assay in fresh medium or ACM. Both fresh medium and ACM include the NC and irisin groups. **(C)** The quantification of migrated cells in HMECs-1, related to **(B)** ( $n = 3$ ).  $*P < 0.05$ . **(D)** Representative images of tube formation in HMECs-1 in fresh medium or ACM. Fresh medium was divided into CoCl<sub>2</sub> and CoCl<sub>2</sub> + irisin groups. ACM included four groups: CoCl<sub>2</sub> ACM, CoCl<sub>2</sub> + irisin ACM (CoCl<sub>2</sub> + irisin), ACM + VEGFA, and CoCl<sub>2</sub> ACM + VEGFA. **(E)** The quantification of tube formation in HMECs-1, related to **(D)** ( $n = 3-4$ ).  $*P < 0.05$ .

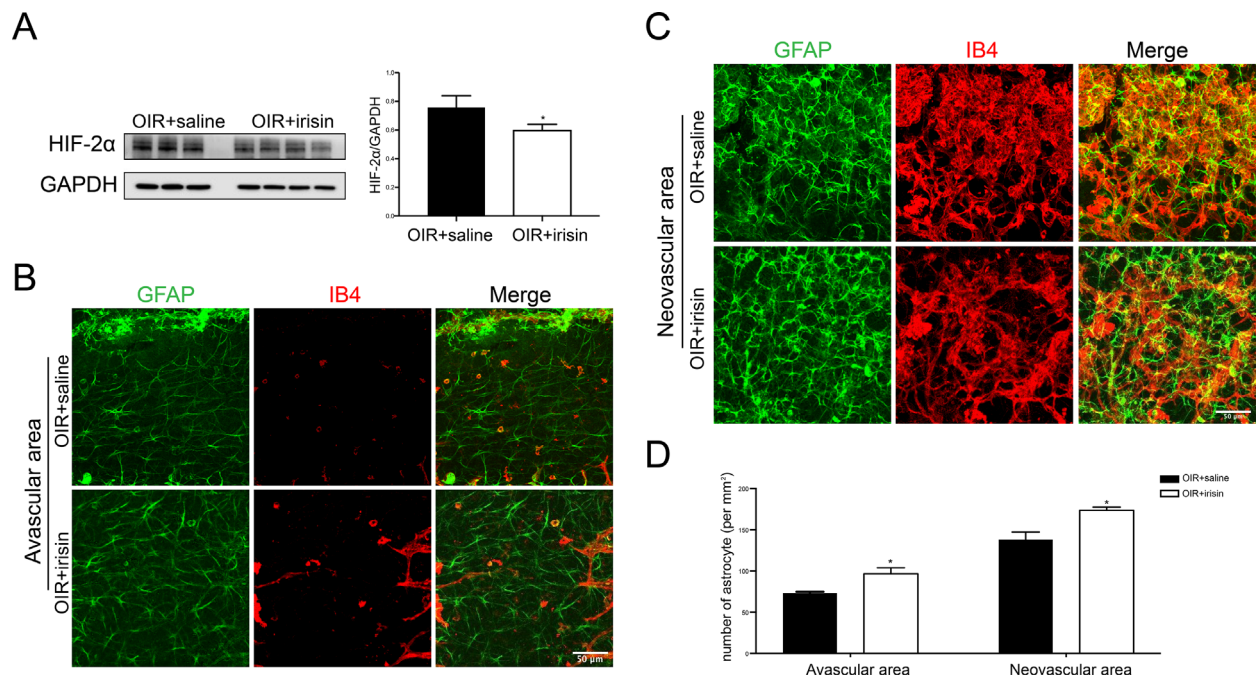


**FIGURE 6.** HIF-2 $\alpha$  expression is reduced in the OIR mice retinae after irisin administration. **(A)** Western blot and quantification of HIF-2 $\alpha$  in the retinae of OIR + saline and OIR + irisin mice at P17 ( $n = 3-4$ ). **(B)** and **(C)** Whole-mount immunostaining with GFAP and IB4 in the avascular and neovascular areas in OIR + saline and OIR + irisin retinae. **(D)** Quantification of the astrocyte density in the avascular and neovascular areas, related to **(B)** and **(C)** ( $n = 3-4$ ).  $*P < 0.05$ .

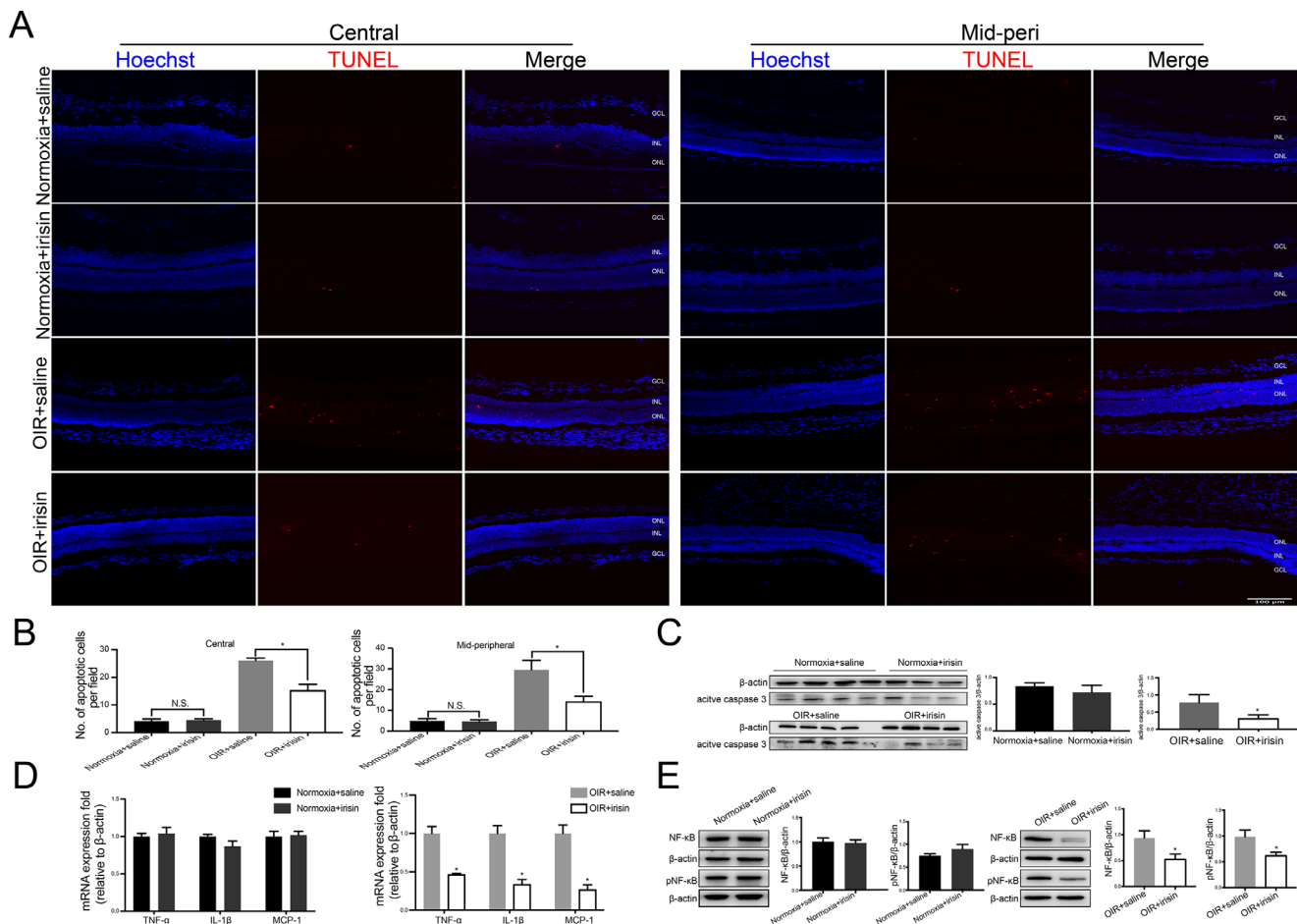


**FIGURE 7.** Irisin prevents cell apoptosis in the OIR retinae. **(A)** Representative images of TUNEL staining in the retinae of normoxia + saline, normoxia + irisin, OIR + saline, and OIR + irisin mice. **(B)** The quantitative analysis of TUNEL-positive cells related to A. **(C)** Western blot analysis and quantification of active caspase 3 expression in normoxia + saline, normoxia + irisin, OIR + saline, and OIR + irisin retinae at P17. **(D)** qPCR analysis of TNF- $\alpha$ , IL-1 $\beta$ , and monocyte chemoattractant protein-1 (MCP-1) mRNA in normoxia + saline, normoxia + irisin, OIR + saline, and OIR + irisin retinae at P17. Data were normalized to the normoxia + saline and OIR + saline groups.  $\beta$ -Actin was used as an internal control. **(E)** Western blot analysis and quantification of NF- $\kappa$ B and pNF- $\kappa$ B protein in the retinae from normoxia + saline, normoxia + irisin, OIR + saline, and OIR + irisin mice upon P17 ( $n = 3-4$ ). \* $P < 0.05$ . GCL, ganglion cell layer; INL, inner nuclear layer; ONL, outer nuclear layer.

compared to the OIR + saline group, with a 1.3-fold increase in the avascular area and a 1.25-fold increase in the neovascular area (Figs. 6B, 6C). Overall retinal images are shown in Supplementary Figure S4. The results suggested that irisin maintained the quantity of astrocytes.

### Irisin Alleviates Apoptosis and Inflammation in the OIR Mice Retinae

Previous studies have demonstrated the beneficial role of irisin in inhibiting apoptosis in many disease models.<sup>41</sup> We also found that the number of TUNEL-positive cells in the retinae was markedly decreased in the OIR + irisin mice compared with the OIR + saline group, with a 42% decrease in the central region and 53% in the midperipheral region. However, irisin made little difference in apoptosis in normoxic mice (Figs. 7A, 7B). Consistently, the expression of active caspase-3, a classical apoptosis-related protein, was lower in the OIR + irisin group (Fig. 7C). Prior studies have witnessed that irisin could act as an anti-inflammatory agent. We further analyzed the effects of irisin on the expression of angiogenesis and inflammation-associated cytokines.

A decreasing trend was found in the expression of TNF- $\alpha$ , IL-1 $\beta$ , and monocyte chemoattractant protein-1 after irisin treatment in the OIR mice (Fig. 7D). NF- $\kappa$ B, an important regulator in angiogenesis, inflammation, and neuron apoptosis, was also examined in our study. The results indicated that both NF- $\kappa$ B and pNF- $\kappa$ B were decreased by irisin administration in OIR, but not in normoxic mice (Figs. 7E).

### DISCUSSION

Neovascular retinal diseases represent a leading cause of blindness globally. The mounting prevalence renders exploring new therapies a matter of urgency. Our present study provided the first evidence that irisin was downregulated in the OIR mice model. Additional irisin mitigated retinal pathological angiogenesis in the OIR mice and decreased VEGFA production in cultured astrocytes. Moreover, irisin suppressed inflammation and neuron apoptosis in the OIR retinae. Mechanistically, irisin decreased the expression of HIF-2 $\alpha$ , NF- $\kappa$ B, and pNF- $\kappa$ B.

Notably, the expression of irisin seems to be downregulated in the OIR retinae. Previous studies showed that circulating and vitreous irisin concentrations were significantly

lower in patients with proliferative DR than in the control group and patients with type 2 diabetes without DR.<sup>27–29</sup> These results suggest that there might be an irisin deficiency in retinal pathological angiogenesis. To investigate the role of irisin, we set out to supplement exogenous irisin in the OIR mice. We found that irisin markedly decreased the avascular and neovascular areas in the OIR retinae. Of note is that VEGFA, which should have been upregulated in the OIR mice, was significantly decreased by irisin. The negative relationship between irisin and VEGFA in the OIR mice is consistent with a former clinical report.<sup>35</sup>

Angiogenesis in the retina is a complex process coordinated by various cells, of which astrocytes play a vital part. Astrocytes are a primary source of VEGFA in retinal pathological angiogenesis.<sup>12,13</sup> An immunofluorescence analysis revealed that irisin notably inhibited astrocyte-derived VEGFA. Consistent with this observation, the lengths and branching points in the superficial layer of retinal vessels decreased significantly. Thus, we speculated that the effect of irisin on pathological angiogenesis might be closely associated with astrocytes. Retinal astrocytes were isolated to investigate the role of irisin in VEGFA production. We found that irisin markedly decreased VEGFA concentration in the medium and VEGFA mRNA and protein expression levels in CoCl<sub>2</sub>-treated astrocytes. Accordingly, conditioned medium from CoCl<sub>2</sub> + irisin pretreated astrocytes suppressed HMECs-1 tube formation, whereas supplementing the missing VEGFA abrogated the inhibitory effects. These data further validated that VEGFA reduction in astrocytes might be responsible for the role of irisin in pathological angiogenesis.

HIF-2 $\alpha$ , a member of the HIF family, plays a vital role in regulating cellular responses to hypoxia.<sup>42</sup> As an essential regulator of VEGFA,<sup>43,44</sup> HIF-2 $\alpha$  was decreased by irisin in CoCl<sub>2</sub>-treated astrocytes. However, blocking the irisin receptor with RGD peptide inhibited irisin-induced HIF-2 $\alpha$  and VEGFA downregulation. In addition, HIF-2 $\alpha$  was also decreased after irisin administration in the OIR mice retinae. These in vitro and in vivo results indicated that irisin might regulate the expression of VEGFA via HIF-2 $\alpha$ . Remarkably, current research showed that HIF-2 $\alpha$  deficiency greatly accelerated retinal astrocyte differentiation.<sup>45</sup> As described, astrocytes provide the scaffold for vascular endothelial migration during retinal vascularization. The astrocytes in contact with the new vessels are mostly immature and own great proliferative capacity. Subsequently, the astrocytes differentiate and express their maturation marker GFAP.<sup>10,46</sup> It has been verified that degeneration of astrocytes in the OIR model leads to disruption of the astrocytic template and pathological angiogenesis eventually.<sup>38,40</sup> Our results showed that irisin inhibited the loss of GFAP-positive astrocytes in the OIR retinae. These findings indicate that irisin might inhibit pathological angiogenesis by targeting HIF-2 $\alpha$ .

Previously, irisin exhibited antiapoptotic and anti-inflammatory properties in a couple of diseases.<sup>41</sup> Similarly, in the current study, irisin exerted an inhibitory role on apoptosis, as demonstrated by reduced TUNEL positive cells and active caspase 3 expression. Nevertheless, neutralizing VEGFA has been reported to cause neuron damage.<sup>47</sup> Thus, irisin may be a better choice for neovascular retinal diseases. A growing body of evidence supports the idea that angiogenesis and inflammation are closely connected. Hong et al.<sup>48</sup> indicated that inflammation could impair retinal angiogenesis in neonatal rats. TNF- $\alpha$ , IL-1 $\beta$ , and monocyte chemoattractant protein-1 mRNA, genes that participate

in angiogenesis and inflammation,<sup>16</sup> showed a remarkable decrease in the OIR mice after irisin injection. Furthermore, irisin decreased the expression of NF- $\kappa$ B and pNF- $\kappa$ B, which are classical regulators in angiogenesis, inflammation, and neuron apoptosis.<sup>16,49</sup>

In conclusion, our study implied for the first time that irisin mitigated retinal neovascularization and preserved neuroglial survival. Still, the present study has intrinsic limitations. First, the origination of irisin is not investigated. Second, further work is needed to elaborate and confirm the detailed mechanism of irisin in OIR. For example, whether irisin could exert an antiangiogenic effect under the administration of an NF- $\kappa$ B agonist or HIF-2 $\alpha$  inhibitor. Furthermore, Guo et al.<sup>50</sup> reported that irisin protects the blood-brain barrier from ischemic injury by decreasing the expression of MMP-9. Whether irisin could preserve the blood-retinal barrier has not been explored.

### Acknowledgments

The authors thank Yuan-Guo Zhou from the State Key Laboratory of Trauma, Burns and Combined Injury, Department of Occupational Disease, Daping Hospital for the constructive suggestions to improve the experiments and our article. The schematic illustrations were created with biorender.com.

Supported by grants from the National Natural Science Foundation of China (No. 82171054 and No. 82000922).

Disclosure: **J. Zhang**, None; **Z. Liu**, None; **H. Wu**, None; **X. Chen**, None; **Q. Hu**, None; **X. Li**, None; **L. Luo**, None; **S. Ye**, None; **J. Ye**, None

### References

- Hartman GD, Lambert-Cheatham NA, Kelley MR, et al. Inhibition of APE1/Ref-1 for neovascular eye diseases: from biology to therapy. *Int J Mol Sci*. 2021;22(19):1354.
- Wang W, LeBlanc ME, Chen X, et al. Pathogenic role and therapeutic potential of pleiotrophin in mouse models of ocular vascular disease. *Angiogenesis*. 2017;20(4):479–492.
- Mca B, Sldbc D. Current perspectives on established and novel therapies for pathological neovascularization in retinal disease. *Biochem Pharmacol*. 2019;164:321–325.
- Singh NK, Kotla S, Kumar R, et al. Cyclic AMP response element binding protein mediates pathological retinal neovascularization via modulating DLL4-NOTCH1 signaling. *EBioMedicine*. 2015;2(11):1767–84.
- Qiu B, Tan A, Veluchamy AB, et al. Apratoxin S4 inspired by a marine natural product, a new treatment option for ocular angiogenic diseases. *Invest Ophthalmol Vis Sci*. 2019;60(8):3254.
- Sankar MJ, Sankar J, Chandra P. Anti-vascular endothelial growth factor (VEGF) drugs for treatment of retinopathy of prematurity. *Cochrane Database Syst Rev*. 2018; 1(5):CD009734.
- Dong X, Lei Y, Yu Z, et al. Exosome-mediated delivery of an anti-angiogenic peptide inhibits pathological retinal angiogenesis. *Theranostics*. 2021;11(11):5107–5126.
- Liu LR, Liu JC, Bao JS, et al. Interaction of microglia and astrocytes in the neurovascular unit. *Front Immunol*. 2020;11:1061.
- Hsiao HY, Chen YC, Huang CH, et al. Aberrant astrocytes impair vascular reactivity in Huntington disease. *Ann Neurol*. 2015;78(2):178–192.
- Selvam S, Kumar T, Fruttiger M. Retinal vasculature development in health and disease. *Prog Retin Eye Res*. 2018; 63(3):1–19.

11. Stenzel D, Lundkvist A, Sauvaget D, et al. Integrin-dependent and -independent functions of astrocytic fibronectin in retinal angiogenesis. *Development*. 2011;138(20):4451–63.
12. Patel C, Narayanan SP, Zhang W, et al. Activation of the endothelin system mediates pathological angiogenesis during ischemic retinopathy. *Am J Pathol*. 2014;184(11):3040–3051.
13. Liu Y, Ji J, Shao W, et al. Bit1-a novel regulator of astrocyte function during retinal development: proliferation, migration, and paracrine effects on vascular endothelial cell. *Hum Cell*. 2019;32(4):418–427.
14. Rossi D. Astrocyte physiopathology: At the crossroads of intercellular networking, inflammation and cell death. *Prog Neurobiol*. 2015;130: 86–120.
15. Ko CY, Chu YY, Narumiya S, et al. CCAAT/enhancer-binding protein delta/miR135a/thrombospondin 1 axis mediates PGE2-induced angiogenesis in Alzheimer's disease. *Neurobiol Aging*. 2015;36(3): 1356–1368.
16. Xu Y, Lu X, Hu Y, et al. Melatonin attenuated retinal neovascularization and neuroglial dysfunction by inhibition of HIF-1 $\alpha$ -VEGF pathway in oxygen-induced retinopathy mice. *J Pineal Res*. 2018;64(4):e12473.
17. Fioravanzo L, Venturini M, Di LR, et al. Involvement of rat hippocampal astrocytes in  $\beta$ -amyloid-induced angiogenesis and neuroinflammation. *Curr Alzheimer Res*. 2010;7(7):591–601.
18. Pignataro P, Dicarolo M, Zerlotin R, et al. FNDC5/irisin system in neuroinflammation and neurodegenerative diseases: update and novel perspective. *Int J Mol Sci*. 2021;22(4):1605.
19. Aydin S, Kuloglu T, Aydin S, et al. Cardiac, skeletal muscle and serum irisin responses to with or without water exercise in young and old male rats: cardiac muscle produces more irisin than skeletal muscle. *Peptides*. 2014;52:68–73.
20. Wrann CD, White JP, Salogiannis J, et al. Exercise induces hippocampal BDNF through a PGC-1 $\alpha$ /FNDC5 pathway. *Cell Metab*. 2013;18(5):649–59.
21. Xin C, Zhang Z, Gao G, et al. Irisin attenuates myocardial ischemia/reperfusion injury and improves mitochondrial function through AMPK pathway in diabetic mice. *Front Pharmacol*. 2020;11:565160.
22. Bi J, Zhang J, Ren Y, et al. Exercise hormone irisin mitigates endothelial barrier dysfunction and microvascular leakage-related diseases. *JCI Insight*. 2020;5(13):e136277.
23. Tu T, Peng J, Jiang Y, FNDC5/irisin: a new protagonist in acute brain injury. *Stem Cells Dev*. 2020;29(9):533–543.
24. Wang K, Song F, Xu K, et al. Irisin attenuates neuroinflammation and prevents the memory and cognitive deterioration in streptozotocin-induced diabetic mice. *Mediators Inflamm*. 2019;2019: 1567179.
25. Hou Z, Zhang J, Yu K, et al. Irisin ameliorates the post-operative depressive-like behavior by reducing the surface expression of epidermal growth factor receptor in mice. *Neurochem Int*. 2020;135(05):104705.
26. Wang K, Li H, Wang H, et al. Irisin exerts neuroprotective effects on cultured neurons by regulating astrocytes. *Mediators Inflamm*. 2018;2018:9070341.
27. Hu WC, Wang R, Ju Li, et al. Association of irisin concentrations with the presence of diabetic nephropathy and retinopathy. *Ann Clin Biochem*. 2016;53:67–74.
28. Tarboush NA, Abu-Yaghi NE, Al Ejeilat LH, et al. Association of irisin circulating level with diabetic retinopathy: a case-control study. *Exp Clin Endocrinol Diabetes*. 2021;129(1):36–42.
29. Zhang C, Ding Z, Lv G, et al. Lower irisin level in patients with type 2 diabetes mellitus: a case-control study and meta-analysis. *J Diabetes*. 2016;8(1):56–62.
30. Madamanchi A, Capozzi M, Geng L, et al. Mitigation of oxygen-induced retinopathy in  $\alpha$ 2 $\beta$ 1 integrin-deficient mice. *Invest Ophthalmol Vis Sci*. 2014;55(7):4338–47.
31. Zudaire E, Gambardella L, Christopher Kurcz, et al. A computational tool for quantitative analysis of vascular networks. *PLoS One*. 2011;6(11):e27385.
32. Di Tomaso MV, Vázquez Alberdi L, Olsson D, et al. Colocalization analysis of peripheral myelin protein-22 and lamin-B1 in the Schwann cell nuclei of Wt and Trj mice. *Biomolecules*. 2022;12(3):456.
33. Duan LJ, Fong GH. Developmental vascular pruning in neonatal mouse retinas is programmed by the astrocytic oxygen-sensing mechanism. *Development*. 2019;146(8):dev175117.
34. Chen DY, Sun NH, Chen X, et al. Endothelium-derived semaphorin 3G attenuates ischemic retinopathy by coordinating  $\beta$ -catenin-dependent vascular remodeling. *J Clin Invest*. 2021;131(4):e135296.
35. Abu-Yaghi NE, Abu Tarboush NM, Abojaradeh AM, et al. Relationship between serum vascular endothelial growth factor levels and stages of diabetic retinopathy and other biomarkers. *J Ophthalmol*. 2020;2020: 8480193.
36. Kang YW, Kim YS, Park JY, et al. Hypoxia-induced apoptosis of astrocytes is mediated by reduction of Dicer and activation of caspase-1. *Cell Biol Int*. 2020;44(6):1394–1404.
37. Wei SS, Bi JB, Yang LF, et al. Serum irisin levels are decreased in patients with sepsis, and exogenous irisin suppresses ferroptosis in the liver of septic mice. *Clin Transl Med*. 2020;10(5):e173.
38. Dorrell MI, Aguilar E, Jacobson R, et al. Maintaining retinal astrocytes normalizes revascularization and prevents vascular pathology associated with oxygen-induced retinopathy. *Glia*. 2010;58(1):43–54.
39. Yun JH, Park SW, Kim JH, et al. Angiopoietin 2 induces astrocyte apoptosis via  $\alpha$ v $\beta$ 5-integrin signaling in diabetic retinopathy. *Cell Death Dis*. 2016;7(2):e2101.
40. Bucher F, Stahl A, Agostini HT, et al. Hyperoxia causes reduced density of retinal astrocytes in the central avascular zone in the mouse model of oxygen-induced retinopathy. *Mol Cell Neurosci*. 2013;56:225–33.
41. Wang Y, Tian M, Tan JY, et al. Irisin ameliorates neuroinflammation and neuronal apoptosis through integrin  $\alpha$ V $\beta$ 5/AMPK signaling pathway after intracerebral hemorrhage in mice. *J Neuroinflammation*. 2022;19(1):82.
42. Jochmanová I, Yang C, Zhuang Z, et al. Hypoxia-inducible factor signaling in pheochromocytoma: turning the rudder in the right direction. *J Natl Cancer Inst*. 2013;105(17):1270–1283.
43. Ahmad A, Ahmad S, Glover L, et al. Adenosine A2A receptor is a unique angiogenic target of HIF-2 $\alpha$  in pulmonary endothelial cells. *Proc Natl Acad Sci USA*. 2009;106(26):10684–10689.
44. Yang F, Liu C, Zhao G, et al. Long non-coding RNA LINC01234 regulates proliferation, migration and invasion via HIF-2 $\alpha$  pathways in clear cell renal cell carcinoma cells. *Peer J*. 2020;8:e10149.
45. Cristante E, Liyanage SE, Sampson RD, et al. Late neuroprogenitors contribute to normal retinal vascular development in a Hif2a-dependent manner. *Development*. 2018;145(8):dev157511.
46. Coorey NJ, Shen W, Chung SH, et al. The role of glia in retinal vascular disease. *Clin Exp Optom*. 2012;95(3):266–281.
47. Beazley-Long N, Hua J, Jehle T, et al. VEGF-A165b is an endogenous neuroprotective splice isoform of vascular

- endothelial growth factor A in vivo and in vitro. *Am J Pathol*. 2013;183(3):918–929.
48. Hong HK, Lee HJ, Ko JH, et al. Neonatal systemic inflammation in rats alters retinal vessel development and simulates pathologic features of retinopathy of prematurity. *J Neuroinflammation*. 2014;11:87–97.
49. Lv S, Cai H, Xu Y, et al. Thymosin  $\beta 4$  induces angiogenesis in critical limb ischemia mice via regulating Notch/NF $\kappa$ B pathway. *Int J Mol Med*. 2020;46(4):1347–1358.
50. Guo P, Jin Z, Wu H, et al. Effects of irisin on the dysfunction of blood-brain barrier in rats after focal cerebral ischemia/reperfusion. *Brain Behav*. 2019;9(10):e01425.